

Fission Characteristics of Individual Deformation Paths in Heavy Elements

Y. L. Zhao,^{*,a,b} I. Nishinaka,^c Y. Nagame,^c K. Tsukada,^c K. Sueki,^b M. Tanikawa,^d S. Goto,^e and H. Nakahara^b

^aInstitute of High Energy Physics, Chinese Academy of Science, Beijing 100039, China

^bTokyo Metropolitan University, Tokyo 192-0397, Japan

^cJapan Atomic Energy Research Institute, Tokai, Ibaraki 319-1195, Japan

^dDepartment of Chemistry, The University of Tokyo, Tokyo 113, Japan

^eDepartment of Chemistry, Niigata University, Niigata, 950-2181, Japan

Received: November 13, 2001; In Final Form: April 3, 2002

The deformation properties of heavy nuclei undergoing the individual fission paths are studied. To understand the nuclear mass division process at low energy, fission events for the symmetric and asymmetric fission paths are analyzed from the overall fission events. The fragment mass-yield distributions for the symmetric and asymmetric fission paths in the fission processes of ²¹⁰Po, ²²⁷Ac, ²³³Pa, ²⁴⁹Bk, and ²⁵⁹Md are systematically studied. Fission characteristics including the deformation of the fissioning nucleus at the scission configuration, the fragment mass-yield distributions, and the total kinetic energy release for individual fission paths are presented.

1. Introduction

Theoretically, multiple fission paths were recently found by the theoretical calculations of the fission potential surface in a five-dimensional deformation space at and beyond the outer saddle points.¹ Experimentally, by examining excitation functions for fission events in the fragment mass distribution and the total kinetic energy (TKE) distribution, we demonstrated the presence of correlations between the saddle-point and scission-point configurations, i.e. the existence of the independent fission paths in the dynamic descent of deforming nuclei from the saddle to scission configurations.² In the lighter actinides, ²³²Th and ²³⁸U, the existence of two independent fission paths has been experimentally certified.² One initiating with the lower threshold energy reaches the less elongated scission configuration leading to the asymmetric mass division and the higher fragment kinetic energy, and the other path starting with the higher threshold energy reaches the elongated scission configuration leading to the symmetric mass division and the lower fragment kinetic energy.

The shape of the mass-yield distribution is one of the long-standing puzzles in fission observations. The observed fragment mass-yield curve was analyzed as a superposition of events originating from different types of the fission process.^{3–7} It has been turned out that these fundamental processes essentially represent the independent fission paths,⁸ or the deformation paths^{9–11} in fission. A recent experiment studying the Coulomb fission of mass-separated radioactive beams unveiled a systematical variation of the shapes of the mass-yield curves from the single symmetric peak to the triple-humped peak and to the double-humped asymmetric peak, for the isotopes of thorium with the change of the neutron number from 132 to 139.¹² In fact, nuclear fission essentially represents an elongation process including many kinds of collective motions of an atomic nucleus. Nuclear mass division occurs at the end (scission configuration) to the dynamic deformation motion of the fissioning nucleus. As mentioned before, the dynamic motions of nuclear matters in the multidimensional space from saddle toward scission points proceed along at least two different paths. The properties of fission fragments are determined by the characteristics of these deformation paths. Accordingly, the experimental informations of each deformation paths of the fissioning nuclei are capable of providing important clues for better understanding the fission properties, such as the mass-yield distribution observed in the experiment. In this context, our present attempt was made to

understand the fission observations from the viewpoint of the characteristics of the individual fission paths.

2. The Deformation Properties of Individual Fission Paths

The measured average $TKE(A_1, A_2)$ value released from a given mass split process is, in first order approximation, equal to the Coulomb repulsion energy between two nascent fragments A_1 and A_2 , i.e. $TKE(A_1, A_2) = Z_1 Z_2 e^2 / D(A_1, A_2)$. Z_1 and Z_2 are the charges for corresponding fragment masses A_1 and A_2 . They were obtained from the UCD model by which the ambiguity being brought into the results was turned out to be about 1%.¹⁰ The $D(A_1, A_2)$ (fm) term is the distance between the charge centers of a pair of complementary fragments at the scission configuration which is the last state for the fissioning nucleus still retaining as a whole. In order to allow an estimation of the degree of deformation at the scission point for different nuclei, a shape elongation β , was defined as $\beta = D(A_1, A_2) / D_0(A_1, A_2)$. Where, $D_0(A_1, A_2) = r_0(A_1^{1/3} + A_2^{1/3})$ with $r_0 = 1.17$, means the distance of two charge centers for the spheres. The β is hence a measure of the degree of the deformation of the scissioning nucleus and an indicator of how much, prior to fission, the nucleus deviates from its spherical shape.

In Figure 1, the measured shape elongations of the scissioning nucleus leading to individual mass splits are displayed as a function of the mass ratio (A_H/A_L) of the pair fragments, in part (a) for fissioning systems ³He + ²³²Th with $E_{He} = 60$ MeV, in part (b) for $p + ^{232}\text{Th}$ with $E_p = 14.7$ MeV, and in part (c) for $p + ^{238}\text{U}$ with $E_p = 14.7$ MeV by solid circles. The data begin from the symmetric center at $A_1 = A_2 = A_f/2$. The plotted data include the fission results of nuclei in the light actinide region, ²³³Pa, ²³⁵U, and ²³⁹Np at the energies ranging from ~ 15 MeV to 60 MeV. On the results of the mass division, fission of 60 MeV ³He + ²³²Th produced a mass-yield distribution having a broad symmetric shape¹³ that represents the typical feature of the symmetric fission process. While fission of $p + ^{232}\text{Th}$ and $p + ^{238}\text{U}$ at $E_p = 14.7$ MeV produced the mass-yield distributions having double-humped peaks that represent the mixture results of coexistence of the both processes of the symmetric and asymmetric mass division. Thus, to understand the nuclear mass division process occurring at the low energy, we need to distinguish the fission events for the symmetric and asymmetric processes from the overall fission events observed.

From the experimental data of solid circles, one sees that in the symmetric mass division region, the observed β of the scissioning nuclei (solid circles around the symmetric mass di-

*Corresponding author. E-mail: zhaoyuliang@ihep.ac.cn.
FAX: +86-(010)-8821-2853.

vision with $A_H/A_L \sim 1$) show a nearly constant value. In the asymmetric mass division region (solid circles in the area of $A_H/A_L > 1.5$), the observed β values of the scissioning nuclei in parts (b) and (c) also remain a nearly constant, but the absolute value is different from that observed in the symmetric mass division region. The question rising here is the β values in between the above two regions are largely varying with the A_H/A_L . They no longer remain the constant nature in between the symmetric and the asymmetric regions of mass divisions. The interpretation for this phenomenon is that fission events in this mass region are produced by more than one type of the fission processes. Under the assumption of the symmetric and asymmetric fission, we decomposed the overall fission events into two components, for the details of the analysis method the reader may refer to Reference 14. It is noted here that this assumption of two fission components does not deny the existence of more fission paths. Two were considered here because the residuals of the fission events after two-component analysis (for the studied fissioning systems) were less than 5% of the total fission. We also tested that adding more fission paths into the analysis did not essentially alter the results presented in this paper.

Open circles and open triangles are the results for the symmetric and asymmetric fission paths, obtained from the analysis of the $TKE(A_1, A_2)$ events using the same analytical method in Reference 14. The data of open circles were determined by the initial parameters for the symmetric fission paths, according to the newly discovered regularity: invariance of the final deformation of fissioning nuclei.⁹ The results of open circles were obtained from the analysis, showing the β values for the asymmetric mass division in the mixture region. One can find that the analytical data (open triangles) in the region of $1.1 < A_H/A_L < 1.5$ show almost identical value with the observed data (solid circles) in the region of $A_H/A_L > 1.5$. This is to say that nuclei undergoing the asymmetric fission path reach a nearly identical scission configuration prior to rupturing into fragments, because the β value is almost unchanged with the change of the mass

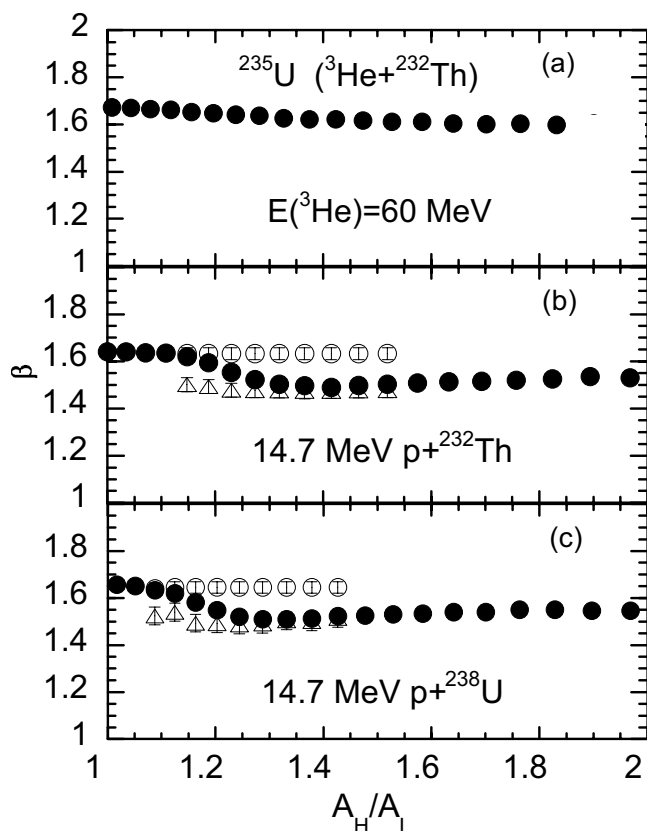


Figure 1. The shape elongations of fissioning nuclei undergoing the symmetric (open circles) and asymmetric (open triangles) fission paths are plotted as a function of the mass ratio of a pair of complementary fragments. The measured data points are indicated via solid circles.

split.

Two remarks need to be noted here. The first, the β values for the nuclei undergoing both the symmetric fission path (see part (a) of Figure 1) and the asymmetric fission path (see parts (b) and (c) of Figure 1) show a slight dependence on the mass split. The β variation of either fission path with the A_H/A_L (in the region of $A_H/A_L = 1.0-2.0$) corresponds to the fluctuation of the TKE ~ 1.5 MeV. This magnitude, may reflect some important information of the fission processes, but unfortunately is within the order of the experimental ambiguity. Therefore, only from the present experimental data, it is difficult to clarify if this variation carries some specific physical significance for the mass division process of the nuclei. The second, the minimum β value in the asymmetric fission path is observed at the mass split leading to the fragment $A = 132$ (corresponding to $A_H/A_L = 1.3$ for $p + {}^{232}\text{Th}$ and 1.25 for $p + {}^{238}\text{U}$ reactions). This may attribute to the presence of the spherical shells $N = 82$ and $Z = 50$ in the fragments, and hence provides the direct evidence for the effects of spherical shells on the final mass division process. In Figure 2(a), the shape elongations for the nuclei undergoing the symmetric fission paths are plotted versus the mass number of the fissioning nucleus. A part of data was reported in References 9, 10, and some new experimental data were added into the present plots. One data point is the β value for one fissioning nucleus as indicated by its name. The data in the area covered by all dot-lines in Figure 2(a) are the β for the fissioning systems with the excitation energy ranging from 10 up to 120 MeV. Skipping such a wide energy region, the fission characteristics show a large variation, but one can find that the β value retains a constant and the variation is as small as less than the vertical height of the shadow space. On the other hand, the β values along the horizontal direction also show a constant nature. It is

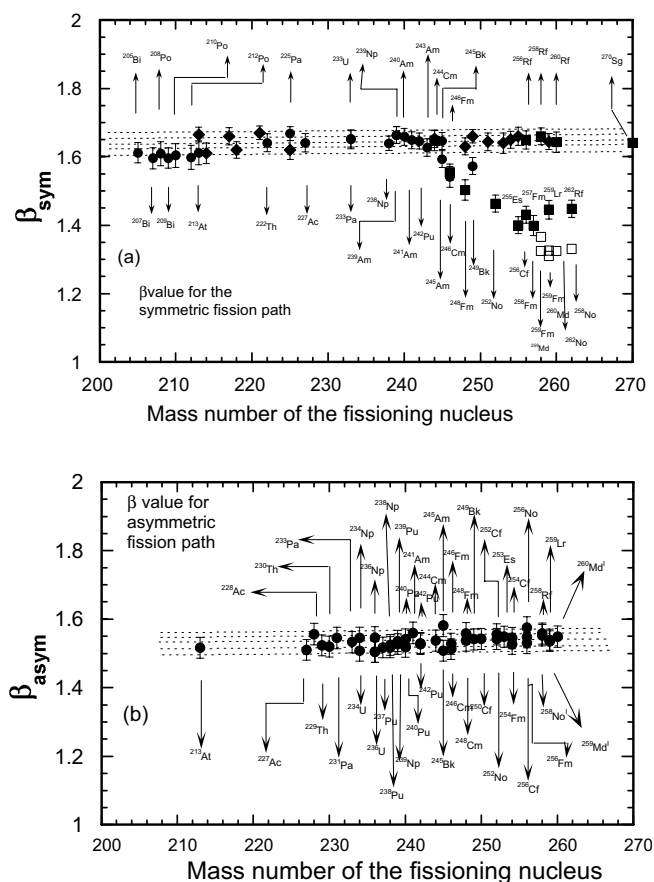


Figure 2. (a) The shape elongations for nuclei at the scission configuration in the symmetric fission path are plotted as a function of the mass number of the fissioning nucleus. (b) The shape elongations for nuclei at the scission configuration in the asymmetric fission path are plotted as a function of the mass number of the fissioning nucleus. The dot-lines marked areas in (a) and (b) indicate the vertical variations of the values.

to say that the final shape elongations of nuclei undergoing the symmetric fission path are nearly the same and not varied with the mass number of the fissioning nucleus, giving the $\beta \sim 1.65$. The data indicated by solid and open squares are the β values for spontaneous fission nuclei in the heavy actinide region. They give different β value from those for the lighter actinide nuclei. This difference in the final deformation of the heavy nucleus ($A_f \sim 260$) and the light nucleus ($A_f < 245$) indicates that the symmetric fission path in the light and heavy actinide is not the same one. From the shape of the fragment mass-yield distribution, it is usually considered that the symmetric fission path nearly vanishes in the region of $A_f \sim 245$, and a sudden change of the fission mode occurs when the nucleus becomes heavier than $A_f = 256$. But the results in Figure 2(a) indicate a smooth transition of the β from $A_f < 245$ with the $\beta \sim 1.65$ to $A_f \sim 260$ with the $\beta \sim 1.33$. No sudden change taking place in the fission processes of nuclei is observed when the nucleus changing from the lighter to heavy actinides.

The data in Figure 2(b) are similar with those in 2(a) but for the asymmetric fission path. Due to some discussions of these results have been made in Reference 9, we hence only mention here some natures that are important for the argument in followings. One may have noticed the identical β values for the asymmetric fission path. All nuclei reach a degree of deformation with a constant $\beta \sim 1.53$ at the scission configuration prior to rupturing into fragments. In conclusion, in the asymmetric fission path the final degrees of the deformation are invariant with the nuclear mass and charge of the fissioning system. The

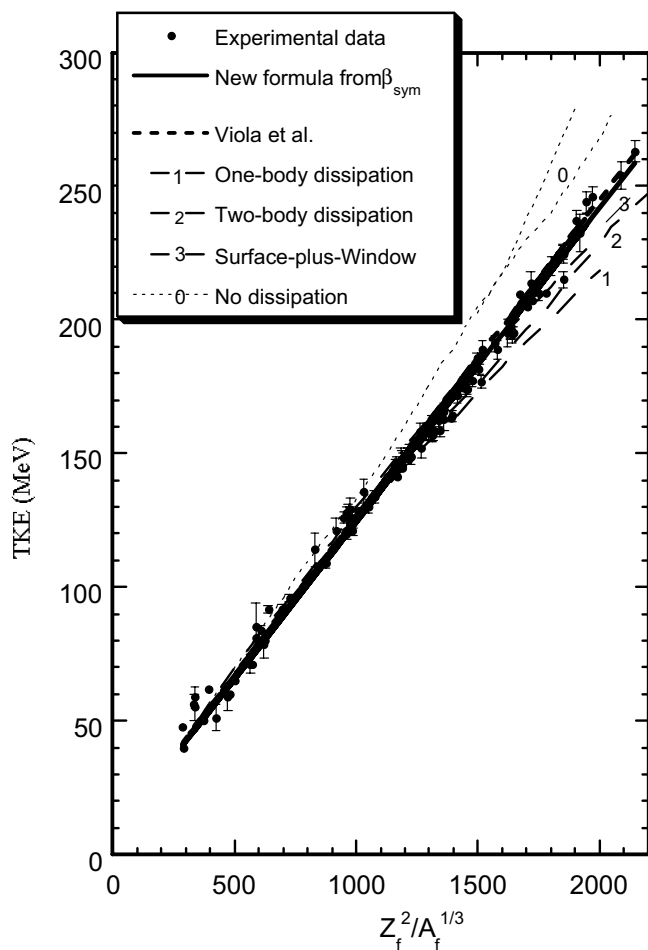


Figure 3. The average total kinetic energies obtained from the experimental measurements (solid circles), the presently derived TKE formula (bold line), Viola's TKE systematics, and theoretical calculations of the dynamic model taking into account one-body dissipation (dashed line with sign "1"), two-body dissipation (dashed line with sign "2"), surface-plus-window dissipation (dashed line with sign "3"), and without dissipation (dashed line with sign "0") are plotted versus the coulomb parameter.

space marked using dot-lines in Figure 2(b) indicates the vertical variation for the β value in the studied A_f -region, it is generally less than 2% of the absolute value.

3. The Total Kinetic Energy Release in Individual Fission Paths

From the identical shape elongation of fissioning nuclei, the formulas for the TKE release in the symmetric and asymmetric fission paths were derived. In the symmetric fission path the constant β of 1.65 gives $\text{TKE} = 0.1173(Z_f^2/A_f^{1/3}) + 7$ MeV, and in the asymmetric fission path the constant β of 1.53 gives $\text{TKE} = 0.1217(Z_f^2/A_f^{1/3}) + 4$ MeV.¹⁴ A comparison of the presently derived TKE function with the available experimental data is given in Figure 3. The experimental data are indicated using solid circles, including the results for the low-energy symmetric fission path and the heavy-ion induced symmetric fission path. The experimental data are taken from References 15–17 and references therein. The new formula (derived from the deformation degree) of the symmetric fission path is shown by the bold line, it is in excellent agreement with the experimental data of solid circles. For comparison, the results of the newest version of Viola's empirical TKE systematics, $0.1187(Z_f^2/A_f^{1/3}) + 7.3$ MeV (Ref. 18) is also indicated by a solid line. It is surprisingly close to the newly derived one for the symmetric fission path. Thus, we can now make a conclusion that the simple linear dependence of the average TKE release in fission on the coulomb parameter $Z_f^2/A_f^{1/3}$ found by Viola et al. essentially originates from the constancy of the shape elongation of the fissioning nucleus at the scission configuration.

In 1980's, Nix and Sierk et al. developed a dynamical model for the nuclear fission process, the dashed lines with the num-

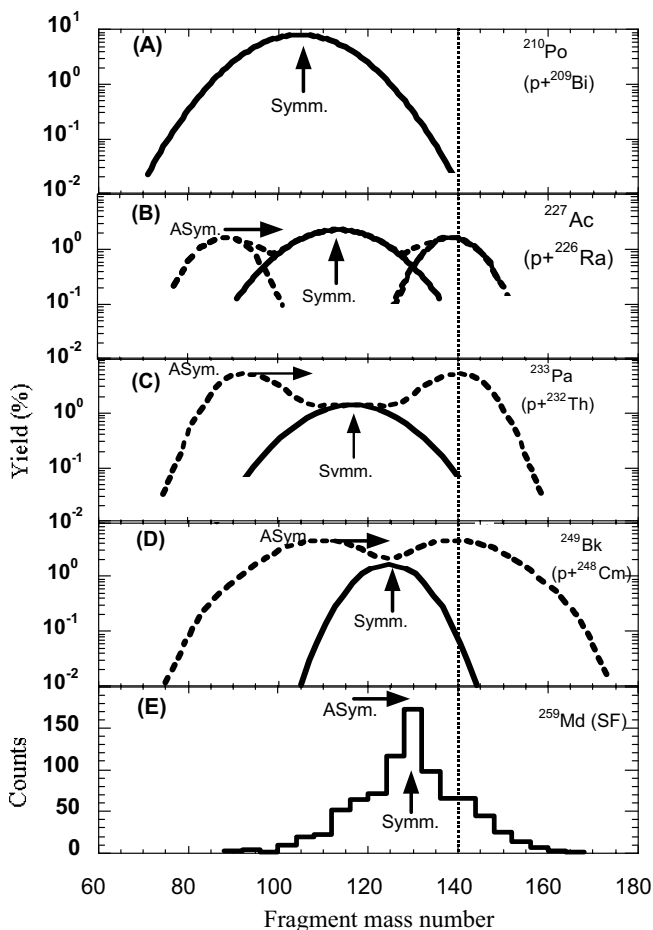


Figure 4. The fragment mass-yield distributions for the representative fissioning nuclei over a large region. They show the smooth, systematic changes in the gross characteristics (such as the shape and peak position) of the mass-yield curve for either of the symmetric and asymmetric fission paths for nuclei from pre-actinide to the heavy actinide.

ber show their theoretical results.¹⁹ In the calculations, effects of several types of the nuclear dissipation force on the dynamical evolution of the fissioning nucleus beyond the fission saddle point were taken into account. The long-dashed line with the sign “1” is the result for the one-body dissipation, that with the sign “2” for the two-body viscosity, that with the sign “3” for the surface-plus-window dissipation. The results calculated without considering any dissipation force are shown via the short-dashed lines with the sign “0”. The theoretical prediction of the dynamical model with the surface-plus-window dissipation shows the best agreement with the experimental data and data obtained from the presently derived TKE formula, except for those in the fission of very heavy nuclei in the region of $Z_f^2/A_f^{1/3} > 1800$.

4. The Fragment Mass-yield Distributions for Individual Fission Paths

On the mass-yield curve, the changing tendency of its shape with the change of the fissioning nucleus in the heavy actinide region was studied in Reference 20. Here we expand our view to a wider region of the fissioning nucleus. In Figure 4, the systematic changes of the mass-yield curve in the fission process of the preactinide ((A) ²¹⁰Po and (B) ²²⁷Ac), and actinide ((C) ²³³Pa, (D) ²⁴⁹Bk, and (E) ²⁵⁹Md) are displayed. The data in parts (C) and (D) for the ²³³Pa and ²⁴⁹Bk are from present measurements. Those in parts (A), (B), and (E) for ²¹⁰Po (Ref. 21), ²²⁷Ac (Ref. 22), and ²⁵⁹Md (Ref. 23) are taken from literature. The corresponding fissioning nuclei and fissioning reactions are indicated in the upper corner of each plot. The solid lines show the mass-yield curves for the symmetric fission path. For ²¹⁰Po, ²²⁷Ac, and ²⁵⁹Md fission, they were obtained from the measurements by experiments. For ²³³Pa and ²⁴⁹Bk, they were gained from the TKE intensities by the analysis method described in Reference 14.

In the following discussions, we will concentrate on the varying trend of the mass-yield curves in the symmetric and asymmetric fission paths. The peak positions of mass-yield curves in the symmetric fission path are marked using a vertical arrow with the letter “Symm”. The peak positions for the light fragment mass in the asymmetric fission path are marked using a horizontal arrow with the letter “Asym”, and those for the heavy fragment mass are marked by a dotted line in the vertical direction.

One sees that for preactinide in ²¹⁰Po region, the nuclei fission symmetrically and produce a broad single peak of the fragment mass-yield curve as the one shown in Figure 4(A). In ²²⁷Ac region, the fission process produces a triple-humped fragment mass-yield curve as the one given in Figure 4(B), where the symmetric and asymmetric fission paths are of the similar importance in determining the results of the nuclear mass division. But as compared to those in the ²¹⁰Po region, the width of the symmetric mass-yield curve becomes narrow. As going into the actinide region, fission of ²³³Pa as well as ²⁴⁹Bk gives out the double-humped fragment mass-yield curves. This is a typical pattern in the actinides. The results of bold lines from the ²¹⁰Po to ²⁴⁹Bk show that the width of the mass-yield curve for the symmetric fission path becomes small with the increase of the mass and charge of the fissioning system. This is probably due to the competition arising from the occurrence of the asymmetric fission path of the dotted lines in Figure 4(B). From the viewpoint of the fission barriers (threshold energies), it has been found that the fission barrier-heights for the symmetric and asymmetric fission paths have the comparable values in the ²²⁷Ac region, while in the actinide the former barrier height becomes higher than the latter.^{24,25}

On the mass-yield curve for the asymmetric fission path, as shown in Figure 4, the light fragment peak of the asymmetric mass-yield curve smoothly moves towards the heavy side when the nucleus becomes heavier in the actinide region. To the con-

trary, the heavy mass peak does not move away as indicated by a vertical dotted line at the fragment mass $A \sim 140$. This phenomenon is turned out to be the same reason¹⁴ leading to the symmetric fragment mass valley to fill in (see gross features of the bold-dashed curves from Figures 4(C) to 4(D)) at the low excitation energy. Previously, this phenomenon was attributed to the decreasing probability for the mass asymmetric fission path with increasing A_f or Z_f in actinide region. But the study of fission probabilities for the individual fission paths based on the precise measurements of the TKE intensities indicated that the relative probability for either of the two paths is nearly constant in the light actinide region. This can be also seen in Figure 4, as the fissioning nucleus becomes heavy, the width of symmetric mass-yield curve becomes narrow and sharp (solid curves), while the height of peak (vertical arrow with “Symm.” sign) becomes lower. In the same time, the asymmetric peak is lowered. But this trend was not observed in the region of heavy actinides, such as in the fission of the ²⁵⁹Md. The reason has been recently revealed¹⁰ from the deformation properties of the nuclei undergoing individual fission paths: the symmetric fission path in the region of the heavy actinide is different from the one in nuclei of the light actinides.

5. Conclusion

As the excitation energy varied in such a large range from 10 to 120 MeV, large variations were observed in the characteristics of fission fragments. But the final degree of deformation of the fissioning nucleus was invariant, giving the $\beta \sim 1.65$ for nuclei in the symmetric fission path and $\beta \sim 1.53$ for those in the asymmetric fission path.

The formulas for the TKE release in the symmetric and asymmetric fission paths, derived from the identical shape elongation of fissioning nuclei, were presented. They are $TKE = 0.1173(Z_f^2/A_f^{1/3}) + 7$ MeV for the former and $TKE = 0.1217(Z_f^2/A_f^{1/3}) + 4$ MeV for the latter. A comparison of the presently derived TKE function with the available experimental data, and the results of the dynamical model calculations taking into account the effects of one-body, two-body, and surface-plus-window dissipations on the dynamical evolution of the fissioning nucleus beyond the fission saddle point indicated that the presently derived TKE formula reproduced well the experimental observations and were in good agreement with the dynamical calculations for the fission of nuclei in the region of $Z_f^2/A_f^{1/3} < 1800$. On the mass-yield distribution, it was found that the varying trend of the gross characteristics in the mass-yield curve was qualitatively correlated to the changing trend of the relative heights of the fission barriers for the symmetric and asymmetric fission paths.

References

- (1) P. Möller, D. G. Madland, A. J. Sierk, and A. Iwamoto, *Nature* **409**, 7858 (2001).
- (2) Y. Nagame, I. Nishinaka, K. Tsukada, Y. Oura, S. Ichikawa, H. Ikezoe, Y. L. Zhao, K. Sueki, H. Nakahara, M. Tanikawa, T. Ohtsuki, H. Kudo, Y. Hamajima, K. Takamiya, and Y. H. Chung, *Phys. Lett. B* **387**, 26 (1996).
- (3) Y. Nagame, I. Nishinaka, K. Tsukada, Y. Oura, S. Ichikawa, H. Ikezoe, Y. L. Zhao, K. Sueki, H. Nakahara, M. Tanikawa, T. Ohtsuki, H. Kudo, Y. Hamajima, K. Takamiya, and Y. H. Chung, *Radiochim. Acta* **78**, 3 (1997).
- (4) Y. Nagame, I. Nishinaka, Y. L. Zhao, K. Tsukada, S. Ichikawa, Z. Qin, H. Ikezoe, Y. Oura, K. Sueki, H. Nakahara, M. Tanikawa, T. Ohtsuki, S. Goto, H. Kudo, Y. Hamajima, K. Takamiya, K. Nakanishi, and H. Baba, *J. Radioanal. Nucl. Chem.* **239**, 97 (1999).
- (5) Y. L. Zhao, T. Ohtsuki, Y. Nagame, I. Nishinaka, K. Tsukada, S. Ichikawa, H. Ikezoe, Y. Hatsukawa, H. Hata,

- M. Tanikawa, K. Sueki, Y. Oura, H. Kudo, and H. Nakahara, *J. Radioanal. Nucl. Chem.* **239**, 113 (1999).
- (6) Y. L. Zhao, Y. Nagame, I. Nishinaka, K. Tsukada, K. Sueki, Y. Oura, H. Nakahara, S. Ichikawa, H. Ikezoe, M. Tanikawa, T. Ohtsuki, and H. Kudo, *J. Alloys Comp.* **271**, 327 (1998).
- (7) M. G. Itkis, N. A. Kondratiev, E. M. Kozulin, Yu. Ts. Oganessian, I. V. Pokrovski, E. V. Prokhorova, and A. Ya. Rusanov, *Phys. Rev. C* **59**, 3172 (1999).
- (8) U. Brosa, H.-H. Knitter, T. S. Fan, J. M. Hu, and S. L. Bao, *Phys. Rev. C* **59**, 767 (1999).
- (9) Y. L. Zhao, I. Nishinaka, Y. Nagame, M. Tanikawa, K. Tsukada, S. Ichikawa, K. Sueki, Y. Oura, H. Ikezoe, S. Mitsuoka, H. Kudo, and H. Nakahara, *Phys. Rev. Lett.* **82**, 3408 (1999).
- (10) Y. L. Zhao, Y. Nagame, I. Nishinaka, K. Sueki, and H. Nakahara, *Phys. Rev. C* **62**, 014612 (2000).
- (11) P. Möller and A. Iwamoto, *Phys. Rev. C* **61**, 047602 (2000).
- (12) K.-H. Schmidt, A. R. Junghans, J. Benlliure, C. Bockstiegel, H.-G. Clerc, A. Grewe, A. Heinz, A. V. Ignatyuk, M. de Jong, G. A. Kudyaev, J. Muller, M. Pfitzner, and S. Steinhauser, *Nucl. Phys. A* **630**, 208c (1998).
- (13) M. G. Itkis, S. M. Luk'yanov, V. N. Okolovich, Yu. E. penionzhkevich, A. Ya. Rusanov, V. S. Salamatin, G. N. Smirenkin, and G. G. Chubaryan, *Yad. Fiz.* **52**, 23 (1990); *Sov. J. Nucl. Phys.* **52**(1), 15 (1990).
- (14) Y. L. Zhao, I. Nishinaka, Y. Nagame, M. Tanikawa, K. Tsukada, K. Sueki, H. Kudo, and H. Nakahara (to be published).
- (15) Y. L. Zhao, Ph.D. Thesis, Tokyo Metropolitan University, 1999, and references therein.
- (16) V. E. Viola, K. Kwiatkowski, and M. Walker, *Phys. Rev. C* **31**, 1550 (1985).
- (17) J. R. Nix and A. J. Sierk, *Nucl. Phys. A* **428**, 161c (1984).
- (18) V. E. Viola, K. Kwiatkowski, and M. Walker, *Phys. Rev. C* **31**, 1550 (1985).
- (19) J. R. Nix, *Nucl. Phys. A* **502**, 609c (1989); Los Alamos National Laboratory, LA-UR-86-698 (1986).
- (20) D. C. Hoffman and M. R. Lane, *Radiochim. Acta* **70/71**, 135 (1995).
- (21) E. Konecny and H. W. Schmitt, *Phys. Rev.* **172**, 1213 (1968).
- (22) M. G. Itkis, V. N. Okolovich, A. Ya. Rusanov, and G. N. Smirenkin, *Z. Phys. A* **320**, 433 (1985).
- (23) E. K. Hulet, J. F. Wild, R. J. Dougan, R. W. Loughheed, J. H. Landrum, A. D. Dougan, M. Schädel, R. L. Hahn, P. A. Baisden, C. M. Henderson, R. J. Dupzyk, K. Summerer, and G. R. Bethune, *Phys. Rev. Lett.* **56**, 313 (1986).
- (24) H. Nakahara and T. Ohtsuki, *J. Radioanal. Nucl. Chem.* **142**, 231 (1990).
- (25) T. Ohtsuki, H. Nakahara, and Y. Nagame, *Phys. Rev. C* **48**, 1667 (1993).